The study of s-process nucleosynthesis based on barium stars, CEMP-s and CEMP-r/s stars

Cui Wenyuan[1,2,3] • **Shi Jianrong**[2] •
Geng Yuanyuan[1] • **Zhang Caixia**[1] •
Meng Xiaoying[1] • **Shao Lang**[1] • **Zhang Bo**[1]*

Abstract In order to get a broader view of the s-process nucleosynthesis we study the abundance distribution of heavy elements of 35 barium stars and 24 CEMP-stars, including nine CEMP-s stars and 15 CEMP-r/s stars. The similar distribution of [Pb/hs] between CEMP-s and CEMP-r/s stars indicate that the s-process material of both CEMP-s and CEMP-r/s stars should have a uniform origin, i.e. mass transfer from their predominant AGB companions. For the CEMP-r/s stars, we found that the r-process should provide similar proportional contributes to the second s-peak and the third s-peak elements, and also be responsible for the higher overabundance of heavy elements than those in CEMP-s stars. Which hints that the r-process origin of CEMP-r/s stars should be closely linked to the main r-process. The fact that some small r values exist for both barium and CEMP-s stars, implies that the single exposure event of the s-process nucleosynthesis should be general in a wide metallicity range of our Galaxy. Based on the relation between C_r and C_s, we suggest that the origin of r-elements for CEMP-r/s stars have more sources. A common scenario is that the formation of the binary system was triggered by only one or a few supernova. In addition, accretion-induced collapse(AIC) or SN 1.5 should be the supplementary scenario, especially for these whose pre-AGB companion with higher mass and smaller orbit radius, which support the higher values of both C_r and C_s.

Cui Wenyuan

e-mail: cuiwenyuan@hebtu.edu.cn

Shi Jianrong

Geng Yuanyuan

Zhang Caixia

Meng Xiaoying

Shao Lang

Zhang Bo*

zhangbo@hebtu.edu.cn

[1]Department of Physics, Hebei Normal University, 20 Nanerhuan Dong Road, Yuhua District, Shijiazhuang 050024, P.R.China.

[2]National Astronomical observatories, Chinese Academy of Sciences, 20A Datun Road, Chaoyang District, Beijing 100012, P.R.China.

[3]Department of Physics, Shandong University, Jinan, Shandong 250100, P.R.China.

1 Introduction

Based on whether the timescale for neutron capture is slower or faster than the β-decay timescale for unstable nuclei, the nuclei beyond the iron group are created in neutron-capture processes, i.e. s- (slow) or r- (rapid). The two neutron-capture processes are thought to occur under different physical conditions and therefore likely to arise in different astrophysical sites. The s-process, which requires a lower neutron flux (with a typical neutron-capture taking many years), is generally thought to occur during the double-shell burning phase of asymptotic giant branch (AGB) stars with low- and intermediate-mass (Busso, Gallino & Wasserburg 1999). The r-process requires a high neutron flux level (with many neutron-captures over a timescale of a fraction of a second), which is expected to take place in the exploding astrophysical site or sites such as the ν-driven wind of Type II (i.e. core-collapse) supernovae (Woosley et al. 1994), the mergers of neutron stars (Rosswog et al. 2000), accretion-induced collapse (AIC; Qian & Wasserburg 2003), and Type 1.5 supernovae (Zijlstra 2004) etc.

Low-mass AGB stars are as well known as the main site for the s-process elements producing (Gallino et al.

1998; Lugaro et al. 2003; Herwig 2004; Käppeler et al. 2011; Bisterzo et al. 2011). During their thermally pulsing (TP) phase of AGB stars, some protons are assumed to penetrate into the top layers of the He-intershell from the bottom of the convective envelope, and then captured by the freshly synthesised ^{12}C then directly producing ^{13}C via the ^{12}C(p, γ) ^{13}N(β^+, ν)^{13}C reactions (Iben et al. 1983). The primary-like reaction, ^{13}C(α, n)^{16}O which works at a temperature of about 0.1×10^9 K, is generally regarded as the major neutron source of the s-process nucleosynthesis. Based on a specific hydrodynamical treatment, Sneden, Cowan & Gallino (2008) pointed out that at the border between the upper H-rich convective envelope and the lower C-rich and He-rich radiative He-intershell, some physical mechanisms such as rotational mixing, shear turbulence, gravitational waves, thermodynamical instability and so on could affect the downflow of protons from the envelope. In fact, the precise mechanism for how protons penetrate into the He-intershell is still unknown. Finally, C and s-elements were brought to the surface of AGB stars from He-intershell by the recurrent third dredge-up (TDU) events. Then, different degrees of abundance enhancement of these elements should be observed, which is related to different initial masses and metallicities.

So far, many metal-poor stars have been found based on some special surveys for metal-poor stars which finished or undergoing now, such as the HK survey (Beers et al. 1992, 2007), the Hamburg/ESO Survey (Christlieb 2003), the Sloan Digital Sky Survey (SDSS) (York et al. 2000), as well as the subprogram of SDSS, i.e. the Sloan Extension for Galactic Understanding and Exploration (SEGUE, Yanny et al. 2009). Where, at least 10% and probably as much as 21% of Galactic stars with [Fe/H]≤ -2.0 were identified as carbon-enhanced metal-poor (CEMP, with [C/Fe]$>$ 1.0) stars (Lucatello et al. 2006; Frebel et al. 2007). Beers & Christlieb (2005) have classified CEMP-stars as CEMP-s, CEMP-r, CEMP-r/s and CEMP no in which no enhanced r- or s-elements observed. These old stars with low initial mass ($M < 0.9M_\odot$) are still on their main-sequence or giant evolution phase. Aoki et al. (2002) reported that about 80% of CEMP-stars are CEMP-s stars which showing high enhancement of s-elements. The plausible scenario for the origin of the C and s-elements of CEMP-stars is usually attributed to mass transfer from their former AGB companions (white dwarfs now) by the stellar wind-accretion in binary systems. It is as well known that Eu is one of the most readily measurable elements in optical spectra of metal-poor stars, which is mainly synthesised through r-process. Actually, Eu is always used

as a represent element of r-process. At present, about half of CEMP-s stars are found with higher Eu enhancement, i.e. CEMP-r/s stars (Sneden, Cowan & Gallino 2008; Käppeler et al. 2011; Bisterzo et al. 2011).

The discovery of CEMP-r/s stars (Hill et al. 2000; Cohen et al. 2003) is puzzling, as their formation requires pollution from both an AGB star and a supernova. The origin of the abundance peculiarities of CEMP-r/s stars is sill a debate issue now, and many scenarios have been presented (see Jonsell et al. 2006, for detail). Qian & Wasserburg (2003) proposed a scenario for the formation of CEMP-r/s stars. In this case, the C and s-process material was firstly produced and then accreted from an AGB primary star, which has evolved to a white dwarf. Then, the white dwarf accretes matter from the secondary one and soon the mass transfer triggered an AIC event. The neutrino wind created by the collapse produces r-process elements, which pollutes the secondary one again. However, it is still far from certain that whether the r-process elements can be produced during AIC. Another possible scenario is that the AGB star transfers s-rich materials to the observed star but does not suffer a large mass loss and at the end of the AGB phase, the degenerate core may reach the Chandrasekhar mass which leading to a Type 1.5 supernova. The reason is due to the low mass-loss rate of AGB star at low metallicity (Zijlstra 2004). Such supernovae could explain both the enhancement pattern and the metallicity dependence of the double-enhanced halo stars. The r-process prepollution is also a possible scenario for CEMP-r/s star formation. In this picture, the formation of binary systems was triggered by a supernova which polluted and clumped a nearby molecular cloud. So, the observed star was firstly enhanced with r-process elements as it once formed, and then received large amounts of s-process elements from its massive AGB companion and finally turned into a CEMP-r/s star (Delaude et al. 2004; Barbuy et al. 2005; Gallino et al. 2005; Ivans et al. 2005). Aoki et al. (2002) proposed that this scenario could possibly explain the formation of CEMP-r/s stars.

Excepting CEMP-s stars, some peculiar red giants with high metallicity similar to the Sun are known as "barium stars", or "BaII stars" which were firstly defined by Bidelman & Keenan (1951). Initially, barium stars only included G and K giants which exhibit enhanced features of BaII, SrII, CH, CN lines and sometimes C_2 molecular bands. Many qualitative studies on barium stars have been developed (e.g. Burbidge & Burbidge 1957; Danziger 1965; Pilachowski 1977; Smith 1984; Začs 1994; Liang et al. 2003; Allen & Barbuy 2006a,b; Smiljanic et al. 2007; Husti et al. 2009). Barium stars could not be self-

enriched, i.e. synthesizing s-process elements in interiors and dredging s-rich materials up to the surface of envelope, because of their lower mass and lower luminosity than those of AGB stars. Periodic variations of the radial velocity have been detected for many barium stars, supporting the scenario that these stars belong to binary systems, and have accreted s-process material from their AGB companions (a white dwarf now) (McClure 1984; McClure & Woodsworth 1990). Dominy & Lambert (1983) and Böhm-Vitense & Johnson (1985) have detected some of their white dwarf companions in the UV with the International Ultraviolet Explorer. Obviously, both barium stars and CEMP-s stars have the similar origin for their enhanced s-elements.

With the help of analysing the abundance patterns of heavy elements enriched stars, the detailed information of s-process nucleosynthesis which taking place in AGB stars can be obtained. In this paper, we focus on the s-process nucleosynthesis at different metallicities, and compare the theoretical yields calculated by our parametric model (Zhang, Ma & Zhou 2006; Cui et al. 2010) with the sample stars. In order to get a broader view about the s-process nucleosynthesis, CEMP-s, CEMP-r/s and barium stars were all included into the sample stars of this work. Moreover, study on the proper sample stars might enable us to directly investigate the products of individual processes, s- and r-process here, and to identify the respective astrophysical sites hoping for r-process. The chosen sample stars are described in Sect. 2, the analysing for the abundance ratios distribution of heavy elements in Sect. 3, and the introduction of the parametric model in Sect. 4. In Sect. 5 the simulation results and the nucleosynthetic effects are discussed, while conclusions are drawn in Sect. 6.

2 Sample Stars

It is well known that the abundances of heavy elements, such as Sr, Ba, Pb, and so on, are enhanced in barium stars ("metal-rich"), CEMP-s and CEMP-r/s stars, which degree just differ by metallicity. Recently, more detailed and more precise abundance data for heavy elements of barium stars have been presented by some works, e.g. Allen & Barbuy (2006a); Pompéia & Allen (2008). In addition, the largest wide-field spectroscopic surveys for metal-poor stars to date and their following high-resolution observations, e.g. the HK survey (Beers et al. 1992) and the HES survey (Christlieb 2003), have provided abundant abundance data with high quality for CEMP-s and CEMP-r/s stars from our

early Galaxy. All of these excellent works make it possible to study the s-process nucleosynthesis at different metallicities by analysing the abundance pattern of heavy elements of sample stars with a wide metallicity range.

It is very important to study such kinds of stars for a better understanding of the efficiency of the s-process at different metallicity in our Galaxy. We explore the pattern of s-process nucleosynthesis with metallicity by comparing the observed abundance of neutron-capture elements with those of the predicted s- and r-process contributions, as the more complete abundance pattern for the neutron-capture elements provides an improved constraint on the nature of the s-process nucleosynthesis. Among barium stars, CEMP-s and CEMP-r/s stars from the literature, we selected only those with all of the following four elements detection, i.e. Sr (or Y for the first s-peak), Ba (for the second s-peak), Eu (for the r-process) and Pb (for the third s-peak). In order to include sample stars as many as possible, some stars with one of the four elements mentioned above, whose upper limit abundance was detected, were also selected. According to this standard, we collected 27 barium stars as displayed in table 1, nine CEMP-s and 15 CEMP-r/s stars as displayed in table 3. In addition, eight barium stars with theoretical values of Pb abundance predicted by Husti et al. (2009) were also included, as there are no observational Pb data available from the literatures.

Spectroscopic data of barium stars were adopted from Allen & Barbuy (2006a); Pompéia & Allen (2008), and Smiljanic et al. (2007), while for the metal-poor stars, the observation data were taken from Aoki et al. (2001, 2002); Johnson & Bolte (2002); Lucatello et al. (2003); Barbuy et al. (2005); Ivans et al. (2005); Jonsell et al. (2006); Cohen et al. (2003, 2006); Goswami et al. (2006); Masseron et al. (2005).

3 The Abundance Ratio Distribution of heavy elements

Elements with $Z > 30$ are labeled in neutron-capture. Though the cumulated content of neutron-capture elements is only about 10^{-6} percent by number of Solar material, but they can produce significant spectral absorption lines, and thus can be detected in stars over a wide metallicity range (Sneden, Cowan & Gallino 2008). So far, many heavy elements have been observed for stars with different metallicity. There are three peaks on the s-process path, i.e. the first s-peak at Sr, Y, Zr (light-s elements, at the neutron magic number N =50), the second s-peak at Ba, La, Ce, etc (heavy-s elements, at N =82) and the third peak at

Pb and Bi (N =126), which locate at the termination point of the s-process path. For convenience, we adopt Ba, La, Ce to represent the heavy-s elements, which is labeled as "hs" hereafter, and Sr, Y, Zr to represent the light-s elements labeled as "ls".

In figure 1, we show, respectively, [Pb/Fe] and [hs/Fe] as a function of [Fe/H] with different symbols employed for barium, CEMP-s, and CEMP-r/s stars. The filled circles represent barium stars, and the red ones represent the one whose lead abundance was predicted by Husti et al. (2009). The unfilled circles represent CEMP-s stars, while unfilled triangles represent CEMP-r/s stars. From figure 1, we can see that both [Pb/Fe] and [hs/Fe] have the same tendency, i.e. increasing with decreasing metallicity, which is consistent with the s-process calculation results of AGB stars with low metallicities (Gallino et al. 1998; Goriely 2000). For the CEMP samples, however, [Pb/Fe] locates in the range of $1.5 - 3.8$ which is almost higher than that of [hs/Fe] ($\sim 0.5 - 2.5$). The standard AGB models, which based on the primary like character of the main neutron source, $^{13}C(\alpha, n)^{16}O$, predict that low-metallicity AGB stars should exhibit higher over-abundances of heavier s-elements ($Z \geq 56$) compared to the lighter ones (such as Sr, Y, Zr, etc). Especially the hugely enhanced Pb and Bi should be attributed to the large number ratios of neutron to iron seeds in low-metallicity environments (Goriely 2000).

Sneden, Cowan & Gallino (2008) pointed out that the s-elements seen in CEMP-s stars should be the result of mass transfer from the winds of AGB companions (the undetected white dwarf now), because nearly all of them are dwarfs or giants with low luminosities, which are much fainter than AGB stars. Many studies on CEMP-r/s and barium stars all agree that the observed overabundance of s-process elements were accreted from the initially more massive star that underwent the AGB phase (Qian & Wasserburg 2003; Barbuy et al. 2005; Gallino et al. 2005; Liang et al. 2003; Allen & Barbuy 2006b; Husti et al. 2009), although the origin of r-enhanced material for CEMP-r/s stars is still in debate (Jonsell et al. 2006). Considering the effect of mass transfer in a binary system, it is difficult to constrain the initial abundances of the s-process synthesis regions from observations of [X/Fe] ratios. Nevertheless, when we study the s-process nucleosynthesis in AGB stars, the mass transfer uncertainty could be canceled if using the abundance ratios, e.g. [Pb/hs] (Straniero, Gallino & Cristallo 2006; Masseron et al. 2010). As the intrinsic indices [Pb/hs] are independent of that whether the s-enhanced star is an intrinsic or extrinsic AGB, it is very useful to investigate the efficiency of the s-process.

In figure 2a,b, we show [Pb/hs] versus [Fe/H] and [Pb/Fe], respectively, the symbols have the same meanings as in figure 1. We can see that the [Pb/hs] values of both CEMP-s and CEMP-r/s stars are almost higher than 0, while, on the contrary, they are almost lower than 0 for barium stars. Moreover, the larger scatter of [Pb/hs] at low-metallicity exists as discussed by Busso et al. (2001) and Käppeler et al. (2011), which are about 2 dex among CEMP-s and CEMP-r/s stars, while 1 dex in barium stars. In addition, although the [hs/Fe] of CEMP-r/s stars is almost higher than that of CEMP-s stars, there are no obviously different in the distribution of [Pb/hs] between these two type stars, which is consistent with the result of Bisterzo et al. (2011). This result proves that the s-process material of both CEMP-s and CEMP-r/s stars should have a uniform origin, i.e. mass transfer from their pre-dominant AGB companions in the corresponding binary systems.

It is interesting that the [hs/Fe] of CEMP-r/s stars is higher than that of CEMP-s stars (see figure 1b), and the abundance ratio [Pb/Fe] shows a similar tendency (see figure 2b), i.e. at a fixed [Pb/hs] value, [Pb/Fe] of CEMP-r/s stars is always larger than that of CEMP-s stars. As it is well known that the neutron-capture elements beyond the iron group are created by some combination of the s- and r-process nucleosynthesis, with each responsible for approximately half of the isotopes. This tendency implies that, excluding the s-process contribution, the r-process of CEMP-r/s stars should contribute to both the second s-peak and the third s-peak elements with similar proportion. Which is also consistent with the proportions of r-process to these elements for their solar abundances, i.e. Ba 15%, La 25%, Ce 19% (second s-peak elements) and Pb 21% (third s-peak elements) (adopted from Burris et al. 2000). In other words, the enhanced over-abundances of heavier s-elements in CEMP-r/s stars than those in CEMP-s stars, such as Pb, Ba, La, etc, should be attributed to r-process nucleosynthesis. Recent studies indicate that the main-r process is responsible for a pure r-process abundance pattern for the heavy r-process elements $56 \leq Z < 83$ (Sneden et al. 2003; Qian & Wasserburg 2007). Montes et al. (2007) suggested that this pattern is remarkably stable from star to star, and in excellent agreement with the contribution of the r-process to the solar abundances. Moreover, the stability of the observed abundance pattern of r-process, and the good agreement with the solar system r-process contribution imply that the r-process events generate a universal abundance distribution, which hints that the r-process origin of CEMP-r/s stars should be closely linked to the main r-process, especially for the elements with $Z \geq 56$.

Figure 3a,b show [ls/Fe] versus [Fe/H] and [hs/ls] versus [hs/Fe], respectively. There is no obvious dis-

tribution difference of [ls/Fe] between CEMP-s and CEMP-r/s stars (see figure 3a). This means that the light-s elements (such as Sr, Y, Zr, etc.) of such two kinds of stars should have a similar origin, i.e. mass transfer from their pre-AGB companions. However, the CEMP-r/s stars almost show higher values of both [hs/ls] and [hs/Fe] than CEMP-s stars. This could be explained by the fact that for the CEMP-r/s stars the r-process have done a large contribution to their heavy-s elements, but a marginal contribution to their light-s elements. In figure 4, we present [N/Fe] versus [C/Fe] for CEMP-s and -r/s stars. The similar distribution of [N/Fe] and [C/Fe] between CEMP-s and -r/s stars also supports that they have suffered an AGB pollution which brought much N, C and s-elements.

Figure 5a shows the abundance ratio [Eu/Fe] versus [Ba/Fe] for CEMP-r/s stars. An obvious correlation between [Eu/Fe] and [Ba/Fe] can be seen from this figure. It is strange that, as we know, Eu and Ba were produced by two independent process (i.e. r- and s-process), respectively. For the formation of CEMP-r/s stars, a popular mechanism is the r-elements pre-enrichment, i.e. r-process material firstly polluted the molecular cloud before the formation of such type stars. It should be noted that the initial r-enrichment does not affect the s-process nucleosynthesis (Bisterzo et al. 2011). To explain this correlation, we have to expect a similar correlation between the dilution event for r- and s-elements during the mass transfer. Allen et al. (2012), however, thought the more reasonable view is that only one process, i.e. the s-process, is responsible for the production of both Ba and Eu, because the AGB stars can produce quite high [Eu/Fe]. In fact, there is a difficulty that whether the s-process could be able to produce a reasonable proportion among the 2nd and 3rd r-peak elements such as Te, Eu, Os, Pt and so on for CEMP-r/s stars (Bisterzo et al. 2012).

We collected here almost all (about 13) r-II stars ([Eu/Fe]>1.0 and [Ba/Eu]<0, see Beers & Christlieb 2005) observed up to now: CS 31082-001 (Plez et al. 2004), CS 22892-052 (Sneden et al. 2003), CS 22183-031 (Hoda et al. 2004), CS 22953-003 (François et al. 2007), CS 29491-069, HE 1219-0312 (Hayek et al. 2009), CS 29497-004, HE 0430-4901, HE 0432-0923, HE 1127-1143, HE 2224+0143, HE 2327-5642 (Barbuy et al. 2005), HE 1523-0901 (Frebel et al. 2007). For comparison, we plot in figure 5b [Eu/Fe] vs. [Fe/H] of these r-II stars and CEMP-r/s stars. From figure 5b, we can see different dependence of [Eu/Fe] on metallicity between CEMP-r/s and r-II stars. [Eu/Fe] of r-II stars decreases with [Fe/H], and reaches a small [Eu/Fe] value (about 1.05) at [Fe/H] ≈ −2.5. The up [Eu/Fe] limit of CEMP-r/s stars, however, still keep a high value (about

1.97) unchanged up to [Fe/H] ≈ −2.0. Furthermore, [Eu/Fe] of r-II stars span a smaller range of [Fe/H], i.e. −3.2 < [Fe/H] < −2.5, than that of CEMP-r/s stars which is from [Fe/H] = −3.1 to −2.0. This means that the r-process responsible for r-II and CEMP-r/s stars should have different physical conditions. The SN II accompanied with r-process maybe have different yields and initial mass. The r-process yields responsible for CEMP-r/s stars should increase with [Fe/H] in order to keep [Eu/Fe] unchanged. For r-II stars, however, the r-process yields of SNII maybe remain stable, the decreasing should be due to the increasing iron abundance in the interstellar medium (ISM hereafter). The different [Fe/H] range of r-II and CEMP-r/s stars maybe is the reason of the small number of r-II stars observed up to now.

4 The Parametric Model

Large samples of s-enhanced stars with wide metallicity ranges, including barium stars, CEMP-s stars, CEMP-r/s stars, can provide a whole information about the nature of s-process. Abundance signatures of heavy elements can help to identify the environment of s-process nucleosynthesis regions (Cowan & Sneden 2006; Sneden, Cowan & Gallino 2008). As the physical mechanism of the proton mixing from the hydrogen-rich envelope to the ^{12}C-rich layer to form a ^{13}C pocket (Busso et al. 2001) is still unknown, the parametric studies are still very useful to explain the formation of s-enhanced stars. In this paper, we adopted an parametric model developed by (Zhang, Ma & Zhou 2006; Cui et al. 2010) to simulate the abundance patterns of barium, CEMP-s and CEMP-r/s stars in order to provide further insight into the nature of s-process nucleosynthesis in the Galaxy.

Four parameters are needed by the parametric model for calculating the s-process nucleosynthesis. They are the neutron exposure per thermal pulse $\Delta\tau$, the overlap factor r, the component coefficient of the s-process C_s and the component coefficient of the r-process C_r, where $\Delta\tau = n_n v_T \Delta t$, and v_T is the average thermal velocity of neutrons at 10^8 K (the appropriate temperature for the ^{13}C$(\alpha, n)^{16}$O reaction working). In this model, the abundance of the ith element in the observed star is calculated as follows:

$$N_i(Z) = C_s N_{i,\ s} + C_r N_{i,\ r} 10^{[Fe/H]}, \qquad (1)$$

where Z is the metallicity of the star, $N_{i,\ s}$ is the abundance of the ith element produced by s-process and $N_{i,\ r}$ is the abundance from r-process, C_s and C_r are

the component coefficients that correspond to contributions from the s-process and the r-process, respectively (see Zhang, Ma & Zhou, 2006 for details).

Barium stars belong to the stellar population I, which were formed in a similar condition with the solar system. In other words, these stars were 'rich' in metallicity as soon as they were formed. Thus, we adopted the scaled solar element abundances based on [Fe/H] of barium stars as the initial abundances of seed nuclei, and the same method were adopted for the initial seed nuclei lighter than the iron peak elements of the CEMP-s and CEMP-r/s stars. In the metal-poor environment, however, the neutron-capture elements in molecular clouds, where CEMP-s and CEMP-r/s stars formed, were mainly produced by r-process. Generally, the r-process abundance pattern of stable neutron-capture elements is divided into two parts, i.e. the r-elements with $Z < 56$ and $Z \geq 56$. The r-elements with $Z \geq 56$ are mainly produced by the main-r process, while the lighter ones are mainly contributed by a light element primary process (LEPP) or/and weak-r process (Travaglio et al. 2004; Kratz et al. 2007; Montes et al. 2007; Cowan et al. 2011). The main-r process produced a stable abundance pattern from star-to-star for elements with $56 \leq Z < 83$, which is consistent with a scaled solar r-process pattern (Montes et al. 2007). Thus, the scaled solar r-process abundance (Arlandini et al. 1999) were adopted as the initial abundance of the heavy elements ($Z \geq 56$). To the light nuclei ($Z < 56$), it is still not clear that whether the r-process pattern is stable from star-to-star, because of the still limited amount of stellar observations for these elements up to now (Cowan et al. 2011). Thus, for the light nuclei we adopted the method suggested by Zhang, Ma & Zhou (2006).

During the calculations, the chi-square (i.e. χ^2) test was also applied in order to get the best simulation results, and the parameters of s-process nucleosynthesis region.

5 Results and Discussion

5.1 Abundance Analysis for Barium Stars

Using the observed abundance data of 35 barium sample stars (Allen & Barbuy 2006a; Smiljanic et al. 2007; Pompéia & Allen 2008), the model parameters can be obtained. The resulted parameters for the neutron exposures per pulse, the overlap factor, the mean neutron exposures and the component coefficients for r- and s-process are listed in Tables 1 and 2.

The best simulation results (solid lines) for each barium star are shown in figure 6, and the observation data (black filled circles) are also plotted for comparing. In figure 6, 26 barium stars are presented as $\log \varepsilon(\mathrm{X})$[1] versus atomic numbers, while the rest nine barium stars are shown as [X/Fe] versus atomic numbers. We can see that the curves calculated by the parametric model, to most stars, agree with the observed abundances well within the error bars. The good agreement of the model results with the observations supports the parametric model we used.

The overlap factor, r, denotes the mass fraction of part material in the s-process nucleosynthesis region, which survived the third dredge-up event and then underwent the succeeding neutron exposure. The r values of the AGB companions of 35 barium stars belong to the range $0.02 \sim 0.39$. There are some stars, such as HD 5424 and HD 107574, whose r values are lower than 0.1, which means that few seed nuclei could experience successive neutron exposure, in other word, the third dredge-up event is very efficient in this case. This situation can be regarded as the so-called single exposure event. Allen & Barbuy (2006b) also obtained a single exposure for HD 5424 and HD 107574 as a best fit to their s-patterns.

In the case of multiple subsequent exposures, the mean neutron exposure is given by $\tau_0 = -\Delta\tau/\ln r$. The mean neutron exposures of the AGB stars, τ_0, corresponding to the 35 barium stars were also shown in tables 1 and 2. In order to compare our results with those of Allen & Barbuy (2006b), we convert our τ_0 values into τ_0^{cha} based on the the formula, $\tau_0^{cha} = \tau_0 \times (T_9/0.348)^{-1/2}$ (where $T_9 = 0.1$, in units of 10^9 K). The results are plotted in figure 7, where τ_0^{All} was taken from Allen & Barbuy (2006b). Based on the definition of τ_0, there is no a real mean neutron exposure in the single exposure mechanism. Thus the mean neutron exposure values relating to 19 barium stars were included in figure 7 for comparing, while seven barium stars were excluded, such as HD 5424, HD 107574, etc, where the single exposure event was responsible for the s-process (see also Allen & Barbuy 2006b). General agreement can be found for our results to those of Allen & Barbuy (2006b), while there are five barium stars, the obvious difference between τ_0^{cha} and τ_0^{All} can be seen. Three of them, i.e. HD 27271, HD 106191, and HD BD+18 5215, the small value 0.05 mbarn^{-1} was calculated based on an exponential exposure under the neutron density 10^{12} cm^{-3} (Allen & Barbuy 2006b), this density is much higher than that of the prediction of Gallino et al. (1998) for the ^{13}C neutron source, while the other two barium stars, i.e. HD 749 and HD 12392, the value of τ_0^{All} is 0.80 mbarn^{-1}, which

---

[1]$\log \varepsilon(\mathrm{X}) = \log(N_X/N_H) + 12$.

is higher than our results, but Allen & Barbuy (2006b) also give 0.406 mbarn^{-1} and 0.40 mbarn^{-1} as values of $\tau_0^{All}(\sigma N)$, those are close to our results, i.e. 0.354 mbarn^{-1} and 0.41 mbarn^{-1}, respectively.

5.2 Abundance Analysis for metal-poor Stars

As mentioned above, our sample include 24 metal-poor stars, i.e. CEMP-s and CEMP-r/s stars here. Among them, 15 stars have been studied in our previous works (Zhang, Ma & Zhou 2006; Cui et al. 2007a,b, 2010), while the other nine stars were simulated in this work using the parametric model. The nucleosynthesis parameters for these nine stars were shown in table 3, and for comparing reason the parameters for the other 15 stars were also presented.

Figure 8 shows our best fits to the observational results of the nine metal-poor stars. The black filled circles with error bars denote the observed element abundances, while the solid lines represent the predictions from s-process calculations, in which the r-process contribution is considered simultaneously. The spectroscopic data adopted from Cohen et al. (2006); Lucatello et al. (2003); Johnson & Bolte (2002); Aoki et al. (2002). We can see that for most stars the calculated results fit with the observed data well within the error bars. The good simulation results suggest that our parametric model is also valid for metal-poor stars.

The r values for most of the metal-poor stars are in the range 0.1 $\sim$ 0.86, while two stars, i.e. HE 1305-0007 and HD 189711, have $r < 0.10$. The lower r value means that only a few seed nuclei can receive the succeeding neutron exposure during the next interpulse phase, in other words, the efficiency of the third dredge-up in their former AGB companions is very high. This case also belongs to the so-called single exposure event. We note this situation is also happened for barium stars as discussed above, thus, we can see that the single exposure event for the s-process nucleosynthesis is general in a wide metallicity range of our Galaxy. Combining the analytical formula of the overlap factor given by Iben (1977) with the initial-final mass relation for AGB stars (Zijlstra 2004), Cui & Zhang (2006) derived a function of r varying with metallicity and initial mass of AGB stars. Using this function, we can find the r range of the AGB stars with initial mass range 1.0 $\sim$ 4.0 M$_\odot$ is very similar with that found in this work excluding the two stars, HE 1305-0007, and HD 189711.

The neutron exposure per pulse, $\Delta\tau$, is also a fundamental parameter in the s-process nucleosynthesis. The calculated values of $\Delta\tau$ vary from 0.23 mbarn^{-1} to 0.88 mbarn^{-1}. We compared the $\Delta\tau$ value with the one we can get from the literature for two stars, LP 625-44 and

LP 706-7. Our values, 0.69 mbarn^{-1} and 0.82 mbarn^{-1} are very close to their ones, 0.71 mbarn^{-1} and 0.80 mbarn^{-1} (Aoki et al. 2001), respectively. The mean neutron exposure (τ_0), here, is even a more important parameter for the s-process nucleosynthesis calculation, whose value mainly dominate the final abundance distribution of the s-process elements in AGB stars. In general, the larger value of τ_0, the more heavier elements can be produced. For example, the lead stars produced in the low metallicity environments where the higher τ_0 exists.

5.3 s-Process Nucleosynthesis Characters at Different Metallicities

In order to get a broader view of the s-process nucleosynthesis, we compare the physical parameters relating to metal-poor stars and barium stars together in the following text, especially to identify the impact of metallicity.

Figure 9 shows r and $\Delta\tau$ versus [Fe/H], respectively. The filled circles represent barium stars, and the unfilled circles represent CEMP-s stars, while the unfilled triangles represent CEMP-r/s stars. We can see that the range of r for metal-poor stars (0.01 $\sim$ 0.86), is larger than that for barium stars (0.02 $\sim$ 0.39). Obviously, the s-process nucleosynthesis is more complicated in metal-poor stars. It should be noted that most r values of our metal-poor samples are larger than 0.40 (see figure 9a). As discussed above, the larger the overlap factor value is, the more iron seeds can receive repeated neutron exposure, which is in favour of heavier elements producing, such as Ba, Pb, etc. Gallino et al. (1998) gave a r range, i.e. $0.40 < r < 0.70$, using their dedicated evolutionary model for AGB stars with initial mass from 1 to 3 $M_\odot$ and metallicity from solar to half solar. Obviously, they are larger than ours for barium stars. Nevertheless, it should be kept in mind that, in Gallino et al.'s model, only 0.05 fraction material can really receive the neutron exposure each time.

From figure 9b, we can see that $\Delta\tau$ value increases with decreasing metallicity, which also support the results of favoring heavier elements production, due to the higher ratio of neutron to iron seeds in low metallicity environment. Mathews, Bazan & Cowan (1992) presented a formula, i.e. $n_n \propto 1/(a + Z/Z_\odot)$, to describe the equilibrium neutron density for the primary neutron source ^{13}C(α, n)^{16}O, where the constant a is roughly given by the ratio of the average neutron-capture cross section times abundance for newly synthesized elements (i.e. so-called primary neutron poisons, such as ^{16}O, ^{14}N, etc.) to the average capture cross section times solar abundance for heavy initial elements, usually $a \sim$

0.001 is adopted. Busso, Gallino & Wasserburg (1999) and Gallino et al. (1999) provided a more simplified relationship between the neutron density and metallicities, i.e. the typical neutron density in the nucleosynthesis zone scales roughly as $1/Z^{0.6}$, for $Z_\odot \geq Z \geq 0.02Z_\odot$. At low metallicities, the effect of the primary poisons prevails. The tendency of neutron density varying with metallicity can be seen clearly from figure 9b. Of course, the neutron exposure time must be considered simultaneously. In addition, no apparent distribution difference between r and $\Delta\tau$ values can be found for both CEMP-s and CEMP-r/s stars.

As we know, τ_0 represents the synthetical effect of r and $\Delta\tau$, and determines the final abundance distribution of heavy elements in AGB stars, thus, it's a more important parameter here. We present $\lg\tau_0$ versus [Fe/H] in figure 10, and a larger scatter exists in $\lg\tau_0$ for CEMP-s and CEMP-r/s stars than that in barium stars can be seen, and the $\lg\tau_0$ values of CEMP-s and CEMP-r/s stars are generally larger than those of barium stars. Obviously, the efficiency of s-process nucleosynthesis responsible for heavy neutron-capture elements of metal-poor samples is higher than that of barium stars. In other words, the more enhanced heavy elements, especially for Pb, can be reached at the lower metallicity environments, which has be proved by the observation data shown in figure 1 and 2, especially, the [Pb/hs] values of metal-poor stars are almost larger than 0, while the barium stars on the contrary. Of course, this could not work at a ultra low-metallicity environment, because the medium- and low-mass stars hadn't evolved to AGB phase, which is thought as the most appropriate site for s-process nucleosynthesis.

From figures 9 and 10 we can see that the three important parameters refer to s-process nucleosynthesis, i.e. r, $\Delta\tau$, τ_0, have similar distribution range in both CEMP -s and CEMP-r/s stars. This supports a uniform origin of the s-process elements for both CEMP-s and CEMP-r/s stars. Moreover, as the τ_0 dominated the final element abundance distribution, the AGB companions should have similar s-process efficiency when τ_0 is analogous. If the r-process contribution were taken away from CEMP-r/s stars, a similar dispersion of abundance ratios, such as [hs/Fe], [Pb/Fe] and [Pb/hs], with CEMP-s stars should be expected. Obviously, the r-process should be responsible for the abundance excess of Ba, Pb, etc. This supports the conclusions derived from the similar proportion of r-process contribution for solar Ba and Pb in section 3. This means that we maybe not need a third process to explain the features of both r- and s-process for CEMP-r/s stars (Lugaro et al. 2012).

For more information, the curves of neutron density (i.e. $\lg N_n$) varying with metallicities given by Gallino et al. (1999) were also plotted in figure 10. Where the dotted line represents the maximum neutron density during the interpulse phase after the first occurrence of TDU, and the solid line for a late interpulse period. The curves have been normalized to the neutron density corresponding to $\tau_0 = 0.152$ mbarn^{-1}, which can give the main s-process component of the solar system using a AGB model with half solar metallicity (i.e. [Fe/H]$\simeq -0.3$). Although there is a large scatter, the tendecy of $\lg\tau_0$ increasing with decreasing metallicities can be seen, which implies that the neutron density plays a more important role in the s-process nucleosynthesis of AGB stars.

The component coefficient of the s-process, C_s, and the component coefficient of the r-process, C_r, versus [Fe/H], are presented in figure 11a,b, respectively. The distribution range of C_s for metal-poor stars is close to that of barium stars (Figure 11a). It's well known that, C_s is related to some important evolution characters of AGB stars, such as structure, efficiency of the TDU, mass of convective envelope, etc. In addition, C_s is also related to the physical parameters of binary system, which the CEMP-s, CEMP-r/s stars or barium stars and their pre-AGB companions belong to, such as the orbital periods, mass accretion efficiency and so on (see the definition of C_s by Zhang, Ma & Zhou 2006; Cui et al. 2007b). Thus, it can be explained that the total dilution efficiency of s-enhanced material from s-process nucleosynthesis region to the star observed now, should be very similar between metal-poor stars and barium stars. In other words, the influence of metallicity is not important on the total dilution efficiency of s-element abundances, which also supports that the s-element enhancement should be resulted by mass transfer from AGB stars for CEMP-s, CEMP-r/s and barium stars. For most of the barium stars, the binarity have been confirmed (McClure 1984; Jeffries & Smalley 1996; Udry et al. 1998a,b).

On the contrary, the C_r values of CEMP-r/s stars are larger than those of CEMP-s and barium stars, because the latter two kinds are s-only stars. The small C_r distribution ranges about $0 - 6.9$ for CEMP-s stars and $0 - 4.3$ for barium stars imply that their r-elements all come from the ISM, where the local polluting event from SN II with r-materials didn't take place recently. While the slightly larger scatter in CEMP-s stars supports the conclusion that the ISM was not mixed well at the early epoch of our Galaxy (Ryan, Norris & Bessell 1991). The large scatter of C_r for CEMP-r/s stars is consistent with the observed large abundance dispersion of the r-elements, such as Eu, Pt etc. However, it is not appropriate that simply regarding CEMP-r/s stars as formed out of r-enriched clouds because of their high

frequency in metal-poor stars (e.g. Aoki et al. 2002). Qian & Wasserburg (2001) also argued that the ISM was sufficiently inhomogeneous to contain such great r-element overabundance relative to Fe at [Fe/H] > −3. This scenario would still be possible, however, if it is modified as that the formation of the binary system is triggered by only one or a few supernova which also provides the r-elements (Gallino et al. 2005; Ivans et al. 2005; Käppeler et al. 2011; Bisterzo et al. 2011). Then, the abundance dispersion could be a natural result from the different r-elements yields of supernova progenitors with different masses. The opinion that the exploding frequency of core-collapse supernovae in early Galaxy is higher enough to explain the observation results of old halo stars, is supported by the chemical evolution model of our Galaxy (Ishimaru & Wanajo 1999; Ishimaru et al. 2004). Although, the chemical inhomogeneities of ISM locally polluted by short-lived massive stars exploding as SN II is often used to explain the r-elements origin of CEMP-r/s stars (Otsuki et al. 2000; Thompson, Burrows & Meyer 2001; Bisterzo et al. 2009; Cui et al. 2010), many arguments on how core-collapse supernovae produce r-process materials still exists (Woosley et al. 1994; Thompson, Burrows & Meyer 2001; Thompson 2003; Wanajo et al. 2002), the AIC-pollution, 1.5 SN-pollution, etc are also possible origins of the r-elements of CEMP-r/s stars (detailed discussion see Jonsell et al. 2006 and references therein).

In figure 12, we plot C_r versus C_s. Obviously, there is no any correlation between C_s and C_r for s-only stars, i.e. CEMP-s and barium stars, while, an obvious positive correlation between C_s and C_r for CEMP-r/s stars as presented in Zhang, Ma & Zhou (2006) exists when more samples included. Zhang, Ma & Zhou (2006) suggested that this imply an increase of s-process matter accreted from the AGB star with increasing r-process matter accreted from the AIC or SN 1.5, which is a significant evidence for the formation scenario of CEMP-r/s stars. Thus, it seems that the AIC and SN 1.5 mechanisms still can not be dismissed, especially for the CEMP-r/s stars with higher C_s value. In fact, the distribution of some fundamental parameters of binary system, such as orbit radius, orbit period, and so on, should be similar in the environments with different metallicities, and the evolution features of AGB stars, such as structure, efficiency of the TDU, mass of convective envelope, and so on, should also be similar for CEMP-s and CEMP-r/s stars with similar metallicity. Thus, the more probable scenario is that many origins of r-elements exist together, i.e. the modified pre-enrichment is a common origin for CEMP-r/s stars, which is sustained by Bisterzo et al. (2011), and AIC or SN 1.5 is supplementary, especially, for whose

pre-AGB companion with higher mass and small orbit radius which support the higher C_r and C_s values, respectively.

Our model is based on the observed abundances of the s-enriched stars and nucleosynthesis calculations, so the uncertainties of those observations and measurement of the neutron-capture cross sections have been involved in the model calculations.

6 Conclusions

We have compared the abundance ratios of heavy elements of 35 barium stars and 24 CEMP-stars including nine CEMP-s and 15 CEMP-r/s stars. The tendency of [Pb/Fe] and [hs/Fe] increasing with decreasing metallicity implies that the environments with lower metallicities are favouring the heavier elements producing, especially for Pb (Gallino et al. 1998; Goriely 2000). And the larger scatter of the efficiency of s-process nucleosynthesis in CEMP-s and CEMP-r/s stars than that in barium stars was found because of lager scatter of their [Pb/hs] ratios, while the similar distribution of [Pb/hs] between CEMP-s and CEMP-r/s stars indicates that the s-process material of both CEMP-s and CEMP-r/s stars should have a uniform origin, i.e. mass transfer from their pre-dominant AGB companions in the corresponding binary systems. Furthermore, for the CEMP-r/s stars, we found that the r-process should provide similar proportional contributions to the second s-peak and the third s-peak elements but marginal contribution to the first s-peak elements if the the s-process contribution were taken away, which should be responsible for the higher over-abundances of heavy elements in CEMP-r/s stars than those in CEMP-s stars. This hints that r-elements origin of CEMP-r/s stars should be closely linked to the main r-process, especially for the elements with $Z \geq 56$.

Based on simulating the abundance distribution of heavy elements of our sample stars, the physical parameters of their corresponding s-process nucleosynthesis were derived. It is found that there are almost larger values of r, $\Delta\tau$ and τ_0 for CEMP-s and CEMP-r/s stars than those for barium stars, which supports the theory that there is higher efficiency for heavier elements producing, especially for Pb, at lower metallicities (Gallino et al. 1998; Goriely 2000). In addition, the fact that some small r values exist for both barium and CEMP-stars, implies that the single exposure event of the s-process nucleosynthesis should be general in our Galaxy. And the similar C_s values between metal-poor and barium stars implies that the total dilution efficiency of s-enhanced material from s-process

nucleosynthesis region to the star observed now, should be very similar for both type stars, i.e. the influence of metallicity is not important on the total dilution efficiency of s-elements abundances. While, the tiny difference of the C_r values between CEMP-s and barium stars, could be explained by the result that all the r-elements come from the ISM, where the local polluting event from SN II with r-materials didn't take place recently, and the ISM was not mixed well at the early epoch of our Galaxy. Combining the larger scatter of C_r values and the positive correlation between C_r and C_s for CEMP-r/s stars, we suggest that the modified pre-enrichment scenario, i.e. the formation of the binary system, which the CEMP-r/s star belongs to, is triggered by only one or a few supernova, which also provides the r-elements, should be the common formation mechanism. And the C_r scatter could be a natural result from the different r-elements yields of supernova progenitors with different masses. In addition, AIC or SN 1.5 should be the supplementary scenario, especially for whose pre-AGB companion with higher mass and smaller orbit radius, which support the both higher C_r and C_s values. Obviously, the fact should be that many origins of r-elements for CEMP-r/s stars exist together.

Clearly, it is important for future studies to determine the r-process sites and the precise r-process yields, which can explain the abundance distribution of r-material in CEMP-r/s stars. More in-depth theoretical and observational studies of CEMP-s and CEMP-r/s stars will reveal more characteristics of the production of r- and s-process elements at low metallicities, and the history of enrichment of neutron-capture elements in our Galaxy.

References

Allen D.M., Barbuy B., 2006a, A&A, 454, 895

Allen D.M., Barbuy B., 2006b, A&A, 454, 917

Allen D.M., Ryan S.G., Rossi S., Beers T.C., Tsangarides S.A., 2012, A&A, 548, 34

Arlandini C., Käppeler F., Wisshak K., Gallino R., Lugaro M., Busso M., Straniero O., 1999, ApJ, 525, 886

Aoki W., et al., 2001, ApJ, 561, 346

Aoki W., Reyan S.G., Norris J.E., Beers T.C., Ando H., Tsangarides S., 2002, ApJ, 580, 1149

Aoki W., Beers T., Christlieb N., Norris J.E., Ryan S.G., Tsangarides S., 2007, ApJ, 655, 492

Barbuy B., Spite M., Spite F., Hill V., Cayrel R., Plez B., Petitjean P., 2005, A&A, 429, 1031

Beers T.C., Preston G.W., Shectman S.A., 1992, AJ, 103, 1987

Beers T.C., Christlieb N., 2005, ARA&A, 43, 531

Beers T.C., Sivarani T., Marsteller B., Lee Y., Rossi S., Plez B., 2007, ApJ, 133, 1193

Bidelman W.P., Keenan P.C., 1951, ApJ, 114, 473

Bisterzo S., Gallino R., Straniero O., Aoki w., 2009, PASA, 26, 314

Bisterzo S., Gallino R., Straniero O., Cristallo S., Käppeler F., 2011, MNRAS, 418, 284

Bisterzo S., Gallino R., Straniero O., Cristallo S., Käppeler F., 2012, MNRAS, 422, 849

Böhm-Vitense E., Johnson H.R., 1985, ApJ, 293, 288

Burbidge E.M., Burbidge G.R., 1957, ApJ, 126, 357

Burris D., Pilachowski C., Armandroff T., Sneden C., Cowan J., Roe H., 2000, ApJ, 544, 302

Busso M., Gallino R., Wasserburg G.J., 1999, ARA&A, 37, 239

Busso M., Gallino R., Lambert D.L., Travaglio C., Smith V.V., 2001, ApJ, 557, 802

Christlieb N., 2003, Rev. Mod. Astron., 16, 191

Cohen J.G., Christlieb N., Qian Y.Z., Wasserburg G.J., 2003, ApJ, 588, 1082

Cohen J.G. et al., 2006, AJ, 132, 137

Cowan J.J., Sneden C., 2006, Nature, 440, 1151

Cowan J.J., Roederer I.U., Sneden C., Lawler J.E., 2011, in RR Lyrae Stars, Metal-Poor Stars, and the Galaxy, ed. A. McWilliam, 223

Cui W.Y., Zhang B., 2006, MNRAS, 368, 305

Cui W.Y., Cui D.N., Du Y.S., Zhang B., 2007a, Chin. Phys. Lett., 24, 1417

Cui W.Y., Zhang B., Ma K., Zhang L., 2007b, ApJ, 657, 1037

Cui W.Y., Zhang J., Zhu Z.Z., Zhang B., 2010, ApJ, 708, 51

Danziger I.J., 1965, MNRAS, 131, 51

Delaude D., Gallino R., Critallo S., Straniero O., Husti L., Ryan S., 2004, Mem. Soc. Astron. Italiana, 75, 706

Dominy J.F., Lambert D.L., 1983, ApJ, 270, 180

François P., Depagne E., Hill V., Spite M., Spite F., Plez B., Beers T.C., Andersen J., James G., Barbuy B., Cayrel R., Bonifacio P., Molaro P., Nordström B., Primas F., 2007, A&A, 476, 935

Frebel A., Christlieb N., Norris J.E., Thom C., Beers T.C., Rhee, J., 2007, ApJ, 660, 117

Gallino R., Arlandini C., Busso M., Lugaro M., Travaglio C., Straniero O., Chieffi A., Limongi M., 1998, ApJ, 497, 388

Gallino R., Busso M., Lugaro M., Travaglio C., Arlandini C., Vaglio P., 1999, in Prantzos N., Harissopulos S., eds, Nuclei in the Cosmos V. Edition Frontières, Paris, p. 216

Gallino R., Delaude D., Husti L., Cristallo S., Straniero O., Ryan S., 2005, Nucl. Phys. A, 758, 485

Goriely S., Mowlavi N., 2000, A&A, 362, 599

Goswami A. et al., 2006, MNRAS, 372, 343

Hayek, W., Wiesendahl, U., Christlieb, N., Eriksson, K., Korn, A.J., Barklem, P.S., Hill, V., Beers, T.C., Farouqi, K., Pfeiffer, B., Kratz, K.-L., 2009, A&A, 504, 511

Herwig F., 2004, ApJS, 155, 651

Hill, V., et al., 2000, A&A, 353, 557

Honda S., Aoki W., Kajino T., Ando H., Beers T.C., Izumiura H., Sadakane K., Takada-Hidai M., 2004, ApJ, 607, 474

Husti L., Gallino R., Bisterzo S., Straniero O., Cristallo S., 2009, PASA, 26, 176

Iben I., 1977, ApJ, 217, 788

Iben I., Renzini A., 1983, ARA&A, 21, 271

Ishimaru Y., Wanajo S., 1999, ApJ, 511, L33

Ishimaru Y. et al., ApJ, 2004, 600, L47

Ivans I.I., Sneden C., Gallino R., Cowan J.J., Preston G.W., 2005, ApJ, 627, L145

Jeffries R.D., Smalley B., 1996, A&A, 315, L19

Johnson J.A., Bolte M. 2002, ApJ, 579, L87

Jonsell K., Barklem P.S., Gustafsson B., Christlieb N., Hill V., Beers T.C., Holmberg J. 2006, A&A, 451, 651

Käppeler F., Gallino R., Bisterzo S., Aoki W., 2011, Rev. Mod. Phys., 83, 157

Kratz K.L., Faroqui K., Pfeiffer B., Truran J.W., Sneden C., Cowan J.J., 2007, ApJ, 662, 39

Liang Y.C., Zhao G., Chen Y.Q., Qiu H.M., Zhang, B., 2003, A&A, 397, 257

Lucatello S. et al., 2003, AJ, 125, 875

Lucatello S., Beers T., Christlieb N., Barklem P.S., Rossi S., Marsteller B., Sivarani T., Lee Y.S., 2006, ApJ, 652, L37

Lugaro M., Herwig F., Lattanzio J.C., Gallino R., Straniero O., 2003, ApJ, 586, 1305

Lugaro, M., Karakas, A.I., Stancliffe, R.J., et al., 2012, ApJ, 747, 2

Masseron T., Van Eck S., Famaey B., Goriely S., Plez B., Siess L., Beers T.C., Primas F., Jorissen A., 2006, ApJ, 455, 1059

Masseron T., Johnson J.A., Plez B., Van Eck S., Primas F., Goriely S., Jorissen A., 2010, A&A, 509, 93

Mathews G.J., Bazan G., Cowan J.J., 1992, ApJ, 391, 719

McClure R.D., 1984, PASP, 96, 117

McClure R.D., Woodsworth A.W., 1990, ApJ, 352, 709

Montes F. et al., 2007, ApJ, 671, 1685

Otsuki T., Tagoshi H., Kajino T., Wanajo S., 2000, ApJ, 533, 424

Pilachowski C.A., 1977, A&A, 54, 465

Plez B., Hill V., Cayrel R., Spite M., Barbuy B., Beers T.C., Bonifacio P., Primas F., Nordström B., 2004, A&A, 428, L9

Pompéia L., Allen D.M., 2008, A&A, 488, 723

Qian Y.Z., Wasserburg G.J., 2001, ApJ, 559, 925

Qian Y.Z., Wasserburg G.J., 2003, ApJ, 588, 1099

Qian Y.Z., Wasserburg G.J., 2007, Physics Reports, 442, 237

Ryan S.G., Norris J.E., Bessell M.S., 1991, AJ, 102, 303

Rosswog S., Davies M.B., Thielemann F.K., Piran T., 2000, A&A, 360, 171

Smiljanic R., Porto de Mello G.F., da Silva L., 2007, A&A, 468, 679

Smith V.V., 1984, A&A, 132, 326

Sneden C., et al., 2003, ApJ, 591, 936

Sneden C., Cowan J.J., Gallino R., 2008, ARA&A, 46, 241

Straniero O., Gallino R., Cristallo S., 2006, Nucl. Phys. A, 777, 311

Thompson T.A., Burrows A., Meyer B.S., 2001, ApJ, 562, 887

Thompson T.A., 2003, ApJ, 585, L33

Udry S., Jorissen A., Mayor M., Van Eck, S. 1998a, A&AS, 131, 25

Udry S., Mayor M., Van Eck S., Jorissen A., Prevot L., Grenier S., Lindgren H., 1998b, A&AS, 131, 43

Wanajo S., Itoh N., Ishimaru Y., Nozawa S., Beers T.C., 2002, ApJ, 577, 853

Travaglio C., Gallino R., Arnone E., Cowan J., Jordan F., Sneden C., 2004, ApJ, 601, 864

Woosley S.E., Wilson J.R., Mathews G.J., Hoffman R.D., Meyer B.S., 1994, ApJ, 433, 229

Yanny B., et al., 2009, AJ, 137, 4377

York D. et al., 2000, ApJ, 120, 1579

Začs L., 1994, A&A, 283, 93

Zhang B., Ma K., Zhou G.D., 2006, ApJ, 642, 1075

Zijlstra A.A., 2004, MNRAS, 348, L23

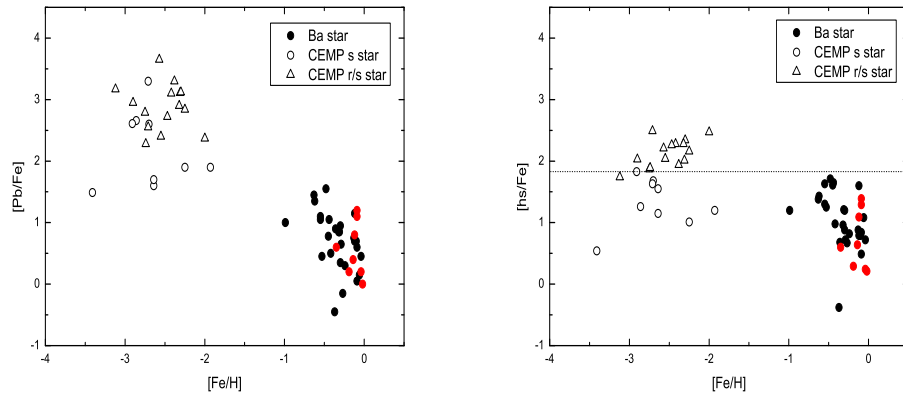**Fig. 1** (a) [Pb/Fe] vs. [Fe/H]; (b) [hs/Fe] vs. [Fe/H]. The filled circles represent barium stars, where the red ones represent the one whose lead abundance was predicted by Husti et al. (2009). The unfilled circles represent CEMP-s stars, and unfilled triangles represent CEMP-r/s stars.
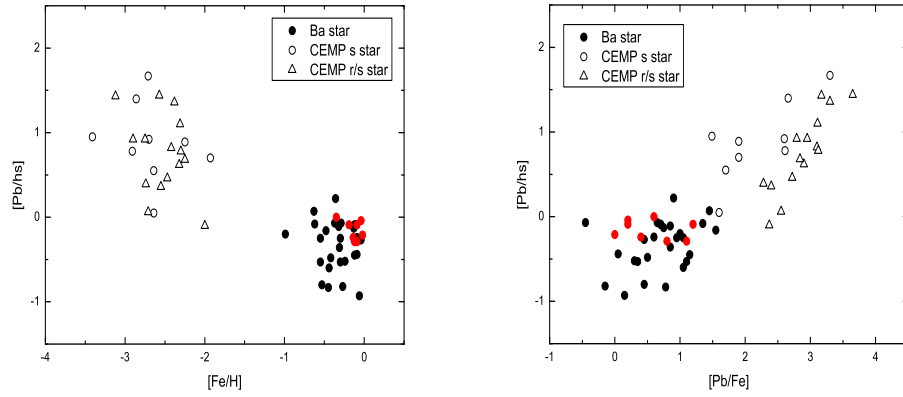

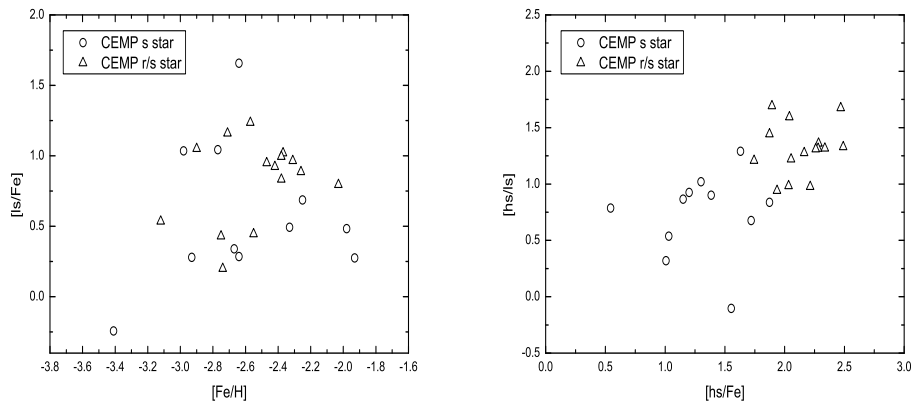**Fig. 2** (a) [Pb/hs] vs. [Fe/H]; (b) [Pb/hs] vs. [Pb/Fe]. The meaning of symbols are same in figure 1.

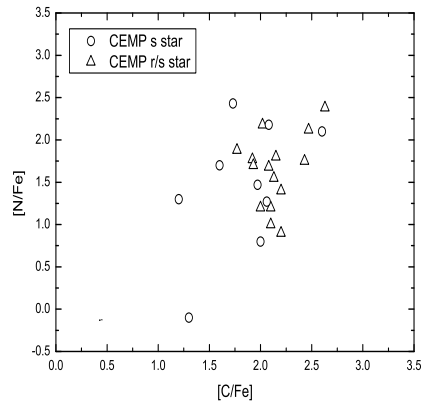**Fig. 3** (a) [ls/Fe] vs. [Fe/H]; (b) [hs/ls] vs. [hs/Fe]. The meaning of symbols are same in figure 1.

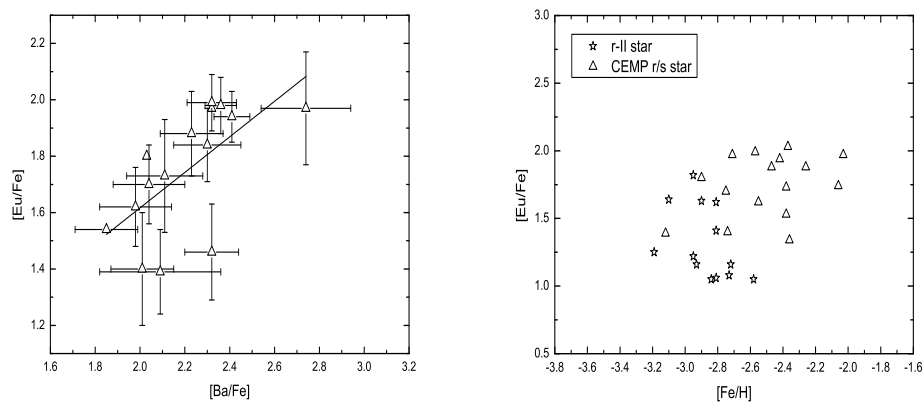**Fig. 4** [N/Fe] vs. [C/Fe]. The meaning of symbols are same in figure 1.

Fig. 5 (a) [Eu/Fe] vs. [Ba/Fe] for CEMP-r/s stars; (b) [Eu/Fe] vs. [Fe/H]. Where the unfilled triangles and stars represent CEMP-r/s and r-II stars, respectively.

Table 1 The derived parameters for the barium stars from Allen & Barbuy (2006a); Pompéia & Allen (2008).

Star	[Fe/H]	$\Delta\tau$ (mb^{-1})	r	τ_0 mb^{-1}	C_s	C_r	χ^2
HR 107	-0.36	0.42	0.10	0.15	0.0043	0.9	1.68534
HD 749	-0.06	0.32	0.18	0.19	0.0017	0.8	7.30354
HD 5424	-0.55	0.52	0.09	0.22	0.0006	1.9	10.52647
HD 8270	-0.42	0.16	0.26	0.12	0.0033	1.7	1.05882
HD 12392	-0.12	0.52	0.10	0.22	0.0003	1.9	10.52035
HD 13551	-0.24	0.16	0.25	0.12	0.0026	0.7	0.62892
HD 22589	-0.27	0.42	0.10	0.18	0.0006	1.5	1.64569
HD 27271	-0.09	0.16	0.25	0.12	0.0022	1.8	2.53701
HD 48565	-0.62	0.33	0.27	0.25	0.0014	0.5	2.41539
HD 76225	-0.31	0.24	0.12	0.11	0.0039	1.2	1.36991
HD 87080	-0.44	0.30	0.33	0.27	0.0008	1.9	4.31905
HD 89948	-0.30	0.26	0.10	0.11	0.0020	1.1	0.97308
HD 92545	-0.12	0.44	0.10	0.14	0.0004	1.9	1.07528
HD 106191	-0.29	0.38	0.10	0.14	0.0007	1.3	1.00532
HD 107574	-0.55	0.48	0.02	0.12	0.0004	2.2	4.76937
HD 116869	-0.32	0.30	0.32	0.26	0.0005	0.9	1.94790
HD 123396	-0.99	0.56	0.16	0.31	0.0003	1.4	13.98755
HD 123585	-0.48	0.26	0.28	0.20	0.0008	4.3	1.50356
HD 147609	-0.45	0.28	0.13	0.14	0.0018	3.7	2.43516
HD 150862	-0.10	0.41	0.10	0.12	0.0007	1.4	1.37586
BD+18 5215	-0.53	0.46	0.10	0.10	0.0012	1.3	2.24078
HD 188985	-0.30	0.30	0.17	0.17	0.0014	1.1	1.47145
HD 210709	-0.04	0.32	0.19	0.19	0.0004	0.9	3.30071
HD 210910	-0.37	0.26	0.17	0.15	0.0006	3.3	2.70146
HD 222349	-0.63	0.31	0.25	0.22	0.0015	0.2	1.28778
HD 223938	-0.13	0.30	0.25	0.22	0.0005	1.0	3.14901
HD 11397	-0.09	0.16	0.39	0.17	0.0011	2.8	0.47400

Table 2 The derived parameters for the barium stars from Smiljanic et al. (2007). References:(a) Present work, (b) Husti et al. (2009).

| Star	[Fe/H]	[Pb/Fe]^a	[Pb/Fe]^b	$\Delta\tau$ (mb^{-1})	r	τ_0 mb^{-1}	C_s	C_r	χ^2
HD 46407	-0.09	0.84	1.1	0.27	0.14	0.14	0.0024	1.7	4.02350
HD 104979	-0.35	0.64	0.6	0.36	0.16	0.20	0.0003	1.3	0.65889
HD 116713	-0.12	0.50	0.8	0.27	0.11	0.12	0.0016	1.9	3.15447
HD 139195	-0.02	-0.24	0.0	0.31	0.05	0.10	0.0004	1.0	0.23194
HD 202109	-0.04	-0.2	0.2	0.25	0.11	0.11	0.0004	0.7	0.25322
HD 204075	-0.09	0.45	1.2	0.27	0.06	0.10	0.0051	0.4	8.53757
HD 205011	-0.14	0.03	0.4	0.25	0.09	0.10	0.0013	0.9	0.86000
HD 181053	-0.19	-0.04	0.2	0.28	0.13	0.14	0.0003	0.3	0.17884
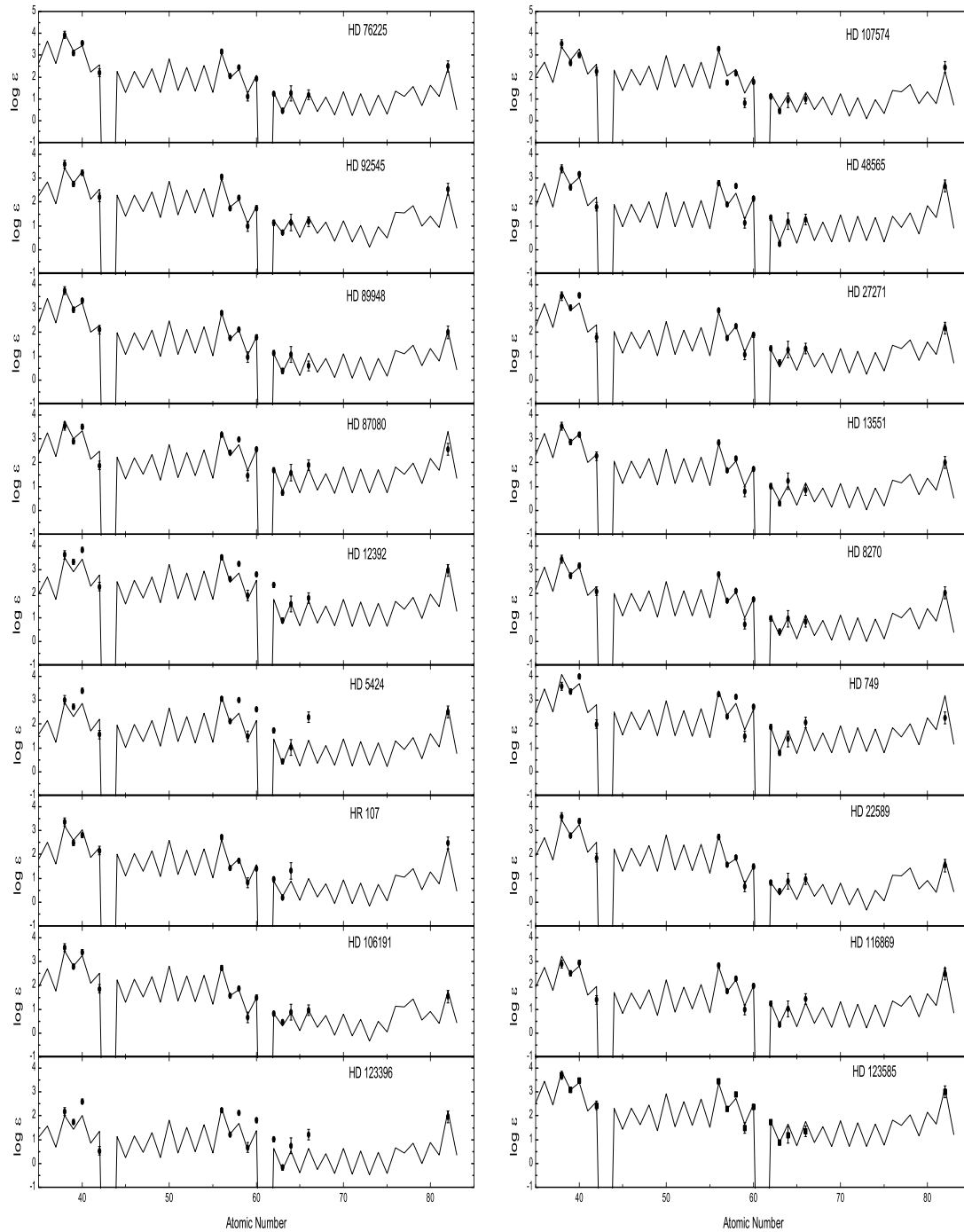
Fig. 6 Best fits to the observational results of barium stars. The filled black circles with appropriate error bars denote the observed element abundances; the solid lines represent predictions from s-process calculations, where the r-process contribution is considered simultaneously. Spectroscopic data adopted from Allen & Barbuy (2006a); Smiljanic et al. (2007); Pompéia & Allen (2008).
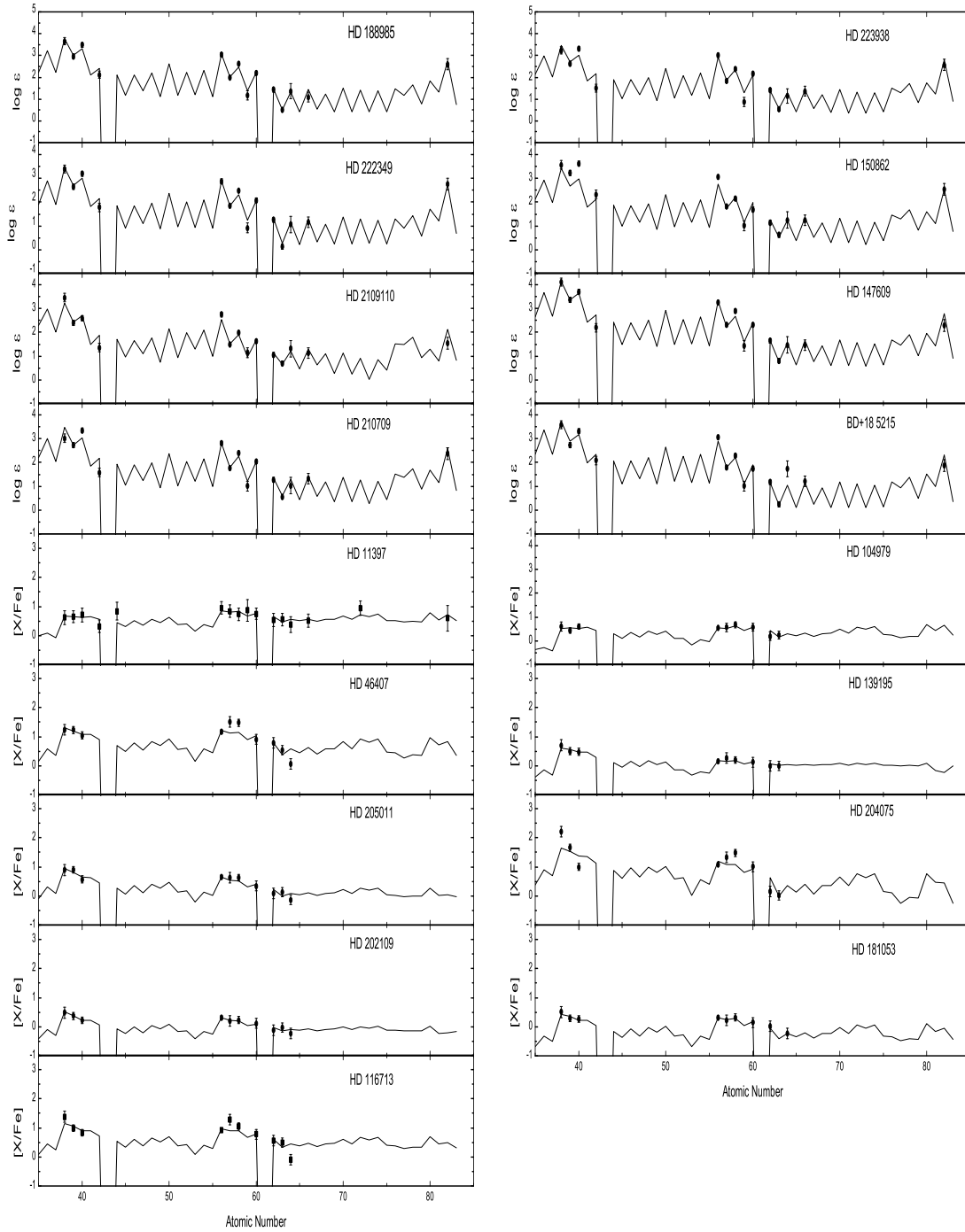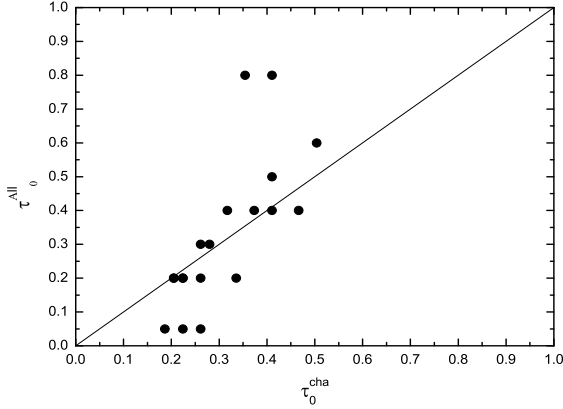
Fig. 6 The rest part of figure 6.

Fig. 7 Comparing the mean neutron exposure of barium stars with results of Allen & Barbuy (2006b).

Table 3 The derived parameters for 24 s-rich metal-poor stars. References: (1) Present work, (2) Cui et al. (2010), (3) Zhang, Ma & Zhou (2006), (4) Cui et al. (2007a), (5) Cui et al. (2007b).

| Star	Class	[Fe/H]	$\Delta\tau$ (mb^{-1})	r	τ_0 mb^{-1}	C_s	C_r	χ^2	ref
HE 0058-0244	rs	-2.75	0.72	0.67	1.80	0.0014	34.6	2.39891	(1)
HE 0143-0441	rs	-2.31	0.68	0.63	1.47	0.0035	18.3	2.19139	(1)
HE 1031-0020	s	-2.86	0.74	0.73	3.46	0.0014	4.6	4.76720	(1)
HE 1509-0806	s	-2.91	0.23	0.73	0.73	0.0031	3.2	0.88808	(1)
HE 2158-0348	s	-2.70	0.52	0.58	0.95	0.0018	3.8	1.73201	(1)
HE 0024-2523	s	-2.71	0.70	0.86	4.64	0.0022	6.9	4.23362	(1)
HE 0338-3945	rs	-2.42	0.76	0.41	0.85	0.0049	63.9	1.00927	(2)
HE 2148-1247	rs	-2.30	0.88	0.10	0.38	0.0045	67.4	2.36022	(3)
HE 1305-0007	rs	-2.00	0.71	0.01	0.15	0.0047	67.4	1.290	(4)
CS 22183-015	rs	-3.12	0.66	0.76	2.40	0.0028	16.7	2.40493	(1)
CS 22880-074	s	-1.93	0.60	0.48	0.82	0.0005	4.7	1.82494	(1)
CS 22942-019	s	-2.64	0.43	0.06	0.15	0.0041	4.7	2.26403	(1)
CS 31062-012	rs	-2.55	0.71	0.32	0.62	0.0018	37.3	0.88371	(3)
CS 31062-050	rs	-2.32	0.71	0.45	0.89	0.0039	60.6	1.02787	(3)
CS 29526-110	rs	-2.38	0.64	0.79	2.72	0.0040	50.6	0.58090	(3)
CS 22898-027	rs	-2.25	0.77	0.42	0.89	0.0035	67.9	1.22539	(3)
CS 22948-027	rs	-2.47	0.61	0.37	0.61	0.0033	65.9	0.40286	(3)
CS 29497-034	rs	-2.90	0.53	0.61	1.07	0.0034	57.3	1.10082	(3)
CS 29497-030	rs	-2.57	0.61	0.81	2.90	0.0060	86.4	2.44198	(3)
CS 30301-015	s	-2.64	0.54	0.34	0.50	0.0005	0.9	1.11864	(3)
CS 30322-023	s	-3.41	0.55	0.65	1.28	0.0002	0.08	0.556	(5)
HD 196944	s	-2.25	0.45	0.44	1.26	0.0006	0.6	0.58686	(3)
LP 625-44	rs	-2.71	0.69	0.16	0.38	0.0045	76.2	2.11142	(3)
LP 706-7	rs	-2.74	0.82	0.10	0.36	0.0017	17.5	0.84623	(3)
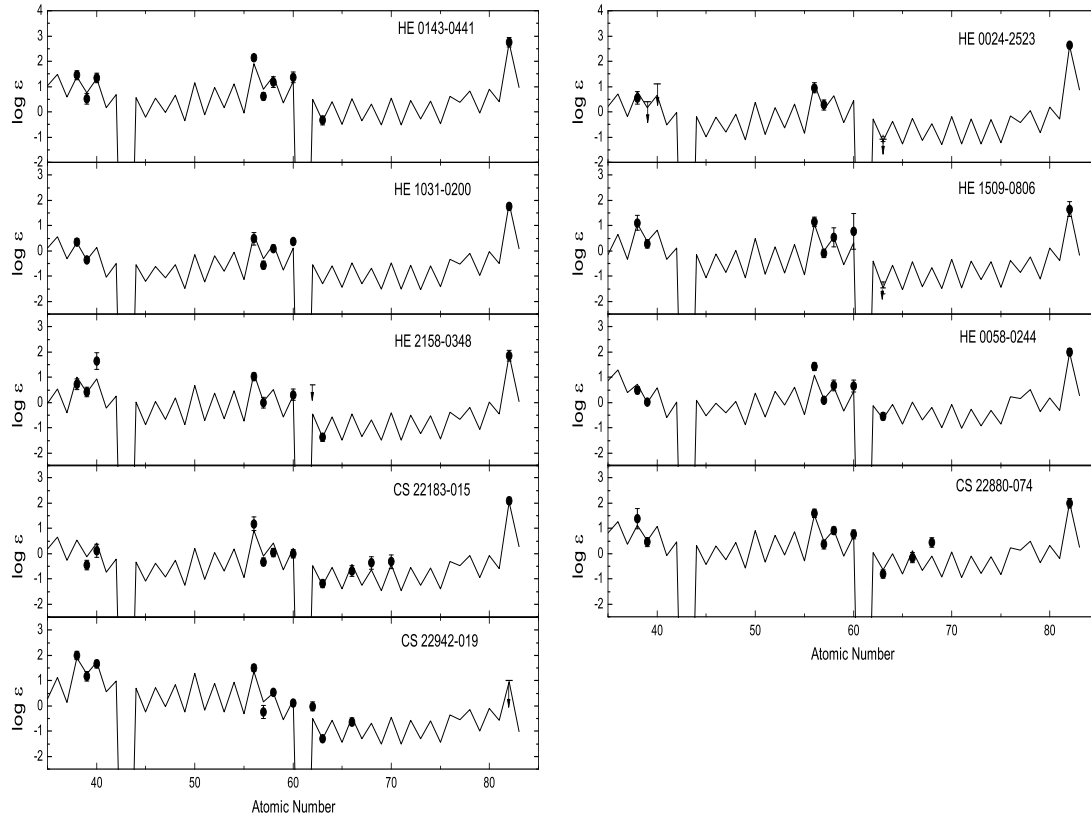
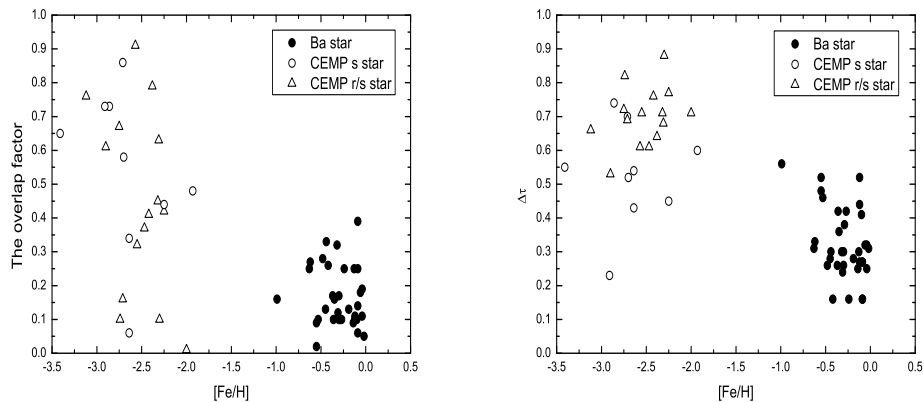**Fig. 8** Best fits to the observational results of metal-poor stars. The symbols are same with figure 6.

Fig. 9 (a) the overlap factor, r, versus [Fe/H]; (b) the neutron exposure per pulse, $\Delta\tau$, versus [Fe/H]. The meaning of symbols are same in figure 1.
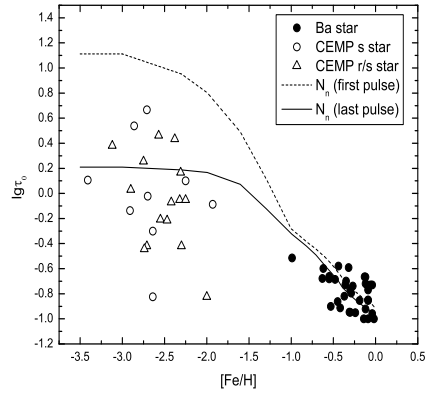
Fig. 10 $\lg\tau_0$ versus [Fe/H]. The meaning of symbols are same in figure 1, except the dotted line for neutron density ($\lg N_n$) after the first TDU, and solid line for the other subsequent neutron density.
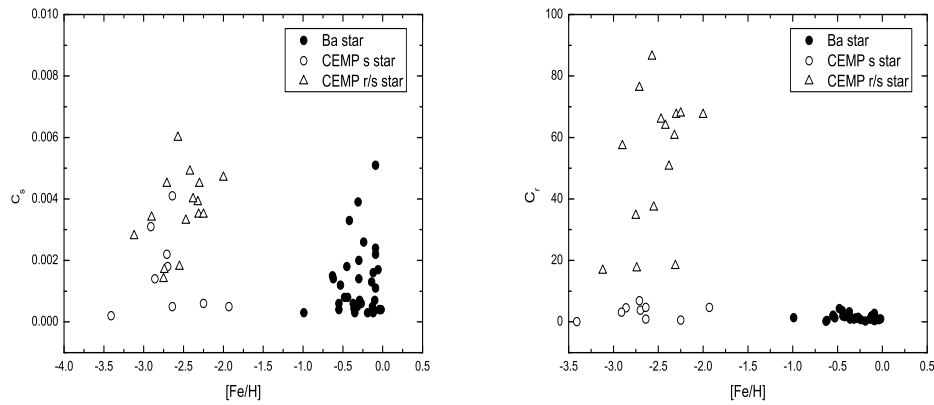

Fig. 11 (a) the component coefficient of the s-process, C_s, versus [Fe/H]; (b) the component coefficient of the r-process, C_r, versus [Fe/H]. The meaning of symbols are same in figure 1.
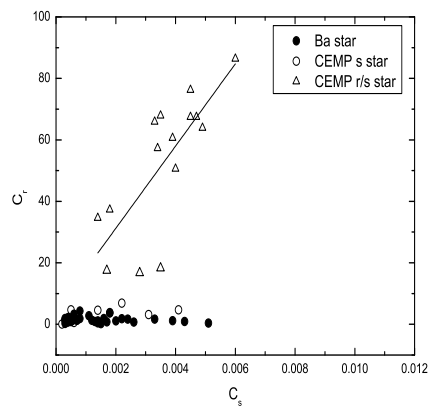
Fig. 12 The relation between C_s and C_r of CEMP-s, CEMP-r/s and barium stars. The meaning of symbols are same in figure 1.